

Fast-Ion Velocity Distributions in JET Measured by Collective Thomson Scattering

H. Bindslev,* J. A. Hoekzema,† J. Egedal,‡ J. A. Fessey, T. P. Hughes,§ and J. S. Machuzak||

JET Joint Undertaking, Abingdon, Oxfordshire, OX14 3EA, United Kingdom

(Received 22 April 1999)

Results on fast ion diagnosis by collective Thomson scattering at JET are presented. 400 kW, 2 mm radiation was scattered in plasmas with energetic proton minority populations heated by 4–8 MW ion cyclotron resonance heating. There is clear evidence of scattering from plasma fluctuations driven by the fast ion population. In a few cases ion velocity distributions with energies in the MeV range could be inferred.

PACS numbers: 52.70.Gw, 52.35.Nx, 52.40.Db, 52.50.Gj

Introduction.—In magnetically confined fusion plasmas, populations of energetic ions are generated by fusion reactions and auxiliary heating. Representing a significant source of free energy ($\approx 1/3$ of plasma energy), the fast ions affect the bulk plasma dynamics, possibly driving modes which can increase transport and lead to prompt fast ion losses [1,2]. Both the interaction of the energetic ions with the bulk plasma and the coupling of radio frequency electromagnetic energy to the fast ions depends crucially on their phase space distribution.

Collective Thomson scattering (CTS) has the potential for mapping out the fast ion phase space distribution by providing spatially localized measurements of the ion velocity distribution with energies into the MeV range [3–8]. The distribution is resolved along a chosen direction in velocity space, determined by the scattering geometry. Both the resolved direction and the spatial location can be varied independently with some constraints. Spatial distribution and velocity anisotropy can thus be studied. This diagnostic capability complements those of other fast ion diagnostics, and is ideal for the study of energetic ion distributions generated by fusion reactions and ion cyclotron resonance heating (ICRH). CTS has been successfully applied to the diagnosis of the bulk ion temperature using a D₂O laser (385 μm) [9] and using millimeter waves generated by gyrotrons [10–14].

At present only CO₂ lasers and gyrotrons are realistic sources of the probing radiation for fast ion CTS. With the wavelengths provided by gyrotrons, the scattering from collective fluctuations dominates for a wide range of scattering angles, giving good spatial localization and flexible scattering geometry [15]. Refraction and electron cyclotron emission (ECE) from the plasma can be significant problems [13,16]. In JET [17] the fast ion CTS signal with a spectral power density on the order of 1 eV had to be detected against a plasma noise background on the order of 1 keV, varying with MHD activity. The CTS signal is discriminated from the noise by modulating the power of the probing radiation.

The first CTS measurements of a distribution of ions with energies in the MeV range are presented here. The results were obtained with the fast ion CTS at JET [11] using 140 GHz, 400, and 100 kW gyrotrons for the prob-

ing radiation. The radiation was modulated at 200 Hz with a duty cycle of 40% for a duration of 0.5 sec in each plasma shot. The probing radiation was launched near the top of the torus and the scattered radiation collected near the bottom. Both transmitter and receiver have steerable, focused, near Gaussian beam, antenna patterns, with a waist radius of 3 cm, giving a spatial resolution of <10 cm in the radial direction. Variable universal polarizers select the elliptical polarizations, required to couple to single plasma modes (*O* or *X*). The detection system was superheterodyne with 32 channels. Notch filters were used to reduce stray radiation. The diagnostic was calibrated using thermal emission from the empty vacuum vessel and ECE [18]. The spectral emissions of the gyrotrons were measured and operating regimes found with sufficient spectral purity [19]. Although the diagnostic could not be fully commissioned in the available experimental time and only a small number of useful shots were recorded (≈ 10), these results nonetheless represent a landmark in the development of fast ion CTS for magnetically confined fusion plasmas. They provide experimental verification of the potential of CTS for fast ion diagnosis.

Raw data.—The CTS signal is extracted by subtracting the noise recorded when the gyrotron is off (ECE period) from the combined noise and signal when the gyrotron is on (gyro period). During switching the gyrotron emits at frequencies not attenuated by the notch filter. To reduce compression of detector gain, the detector is blocked with a pin switch in these periods (pin period). The noise is principally due to electron cyclotron emission (ECE) from the plasma (100–2000 eV), detector noise (≈ 100 eV in most channels), and low frequency electrical pickup. The ECE level varies from shot to shot depending on magnetic field, plasma shape, and electron temperature, and during a shot because of MHD activity.

Figure 1 shows the calibrated signal recorded in a channel on the edge of the bulk ion feature. MHD activity causes large variations in the ECE intensity on short time scales. These encumber the extraction of the CTS signal. The jump in the ECE level at 0.225 sec is due to a sawtooth collapse, which results in an increase in electron temperature outside the inversion radius where the ECE in this frequency band originates from. Samples recorded

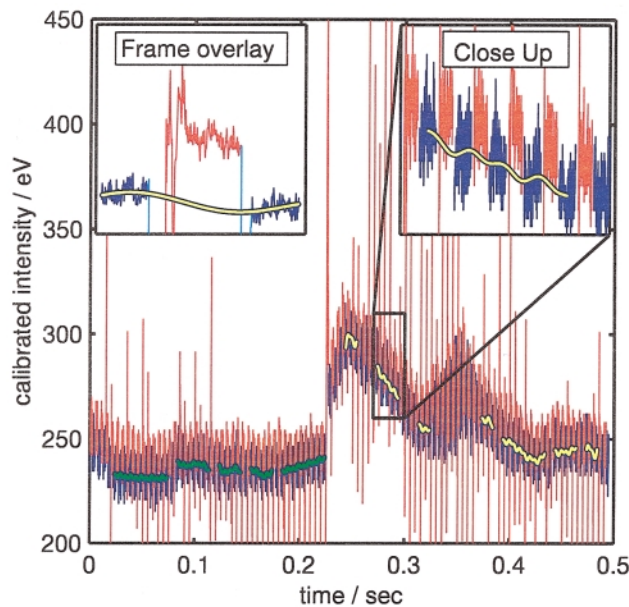


FIG. 1 (color). Raw data. During red gyro periods the gyrotron is on. In blue ECE periods the gyrotron is off. In cyan periods the detector is blocked by a pin switch. Green and yellow curves are fitted to the raw data in the ECE periods and used to estimate the noise in the gyro periods. The extent of the green and yellow curves indicates the selected frames (gyrotron modulation cycles) where MHD activity is tolerable. Also shown is a close-up, and an overlay of the 24 selected frames taken after the sawtooth collapse. A frame lasts 5 ms. The data were recorded 12.5 to 13.0 sec after breakdown.

during enhanced MHD activity are eliminated by a selection criterion which requires that the variance of the signal in pairs of ECE periods does not deviate from the mean variance, and the variance of the neighboring ECE periods, by more than set factors. The result of this *MHD data filtering* for the data recorded before and after the sawtooth collapse is shown in Fig. 1 by the green and yellow curve segments which extend over the selected data. The eliminated data around 0.35 sec coincide with the presence of a 3 kHz modulation of the ECE.

MHD induced variations in the ECE intensity on longer time scales are still present. In addition there is a spurious pickup at 100 and 200 Hz. Attempts at eliminating this during the campaign were not successful. To minimize the effect of both we use as estimates of noise during gyro periods the green and yellow curves, which are fitted to the data recorded in the ECE periods.

The data recorded over a cycle of the gyrotron modulation is a frame. Overlaying frames (averaging over values at identical relative times within a frame) the scatter is reduced and the CTS signal brought out more clearly. With a frame frequency of 200 Hz, the overlay also reduces the 100 Hz pickup but not the 200 Hz pickup. The result of overlay of frames selected after the sawtooth collapse is shown in the inset in Fig. 1.

The large variations in signal at the beginning of the gyro periods are due to residual spurious modes emitted by the gyrotron at frequencies not attenuated by the notch filter.

This leads to increased signals when a mode frequency falls within a channel, and otherwise to depressed signals due to amplifier compression.

The CTS signal is estimated as the difference between the signal and the fit in the gyro periods. To reduce the effects of spurious gyrotron modes and drift of the main gyrotron frequency we use only the last two-thirds of the gyro periods for estimating the CTS spectra.

Spectra and distributions.—Figure 2 shows the CTS spectrum received from plasma shot 44198 in the 0.24 sec following the sawtooth collapse at 0.225 sec (12.725 sec after breakdown), using the 24 selected frames indicated in Fig. 1. The total CTS signal integration time was $\tau = 30$ ms. For comparison we give in the same figure the spectrum recorded for shot 44195 where plasma breakdown was not sustained and the probing radiation thus launched into vacuum while most systems were activated. With a spectral power density of 1 to 5 eV in the *fast ion feature* of shot 44198 as compared with fluctuations of ± 0.1 eV around zero for 44195, it is clear that the signals recorded for shot 44198 are affected by the presence of plasma. We attribute the signals to collective Thomson scattering (CTS) from microscopic fluctuations driven primarily by ions. The signals in the most central 4 channels are mainly due to the ions with thermal velocities (bulk ions), while the rest are principally due to the fast ions

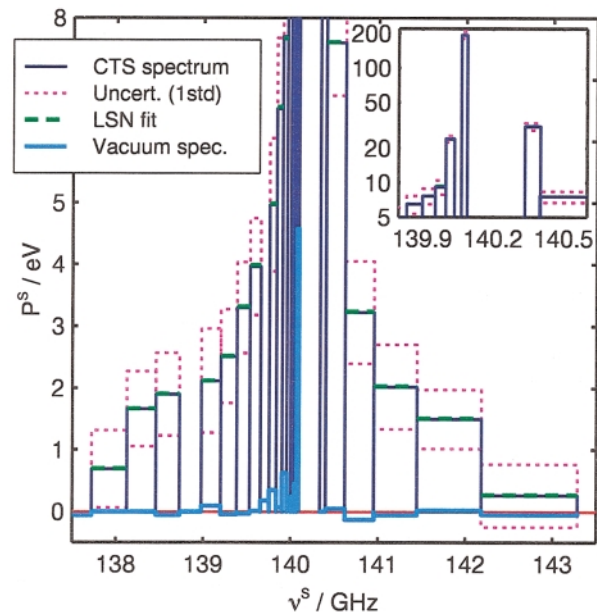


FIG. 2 (color). (Shot 44198.) Recorded spectrum when 400 kW rf was launched into a JET plasma with an ICRH generated fast proton population. $P_{ICRH} = 4$ MW. $n_e = 3.3 \times 10^{19} \text{ m}^{-3}$, $T_e = 3.3$ keV, $T_i = 3.0$ keV, $\theta = 19.3^\circ$, $\phi = 102^\circ$, $T = 0.24$ s, $\tau = 30$ ms. Inset shows spectral density in central channels. The thin magenta dashed bars indicate uncertainty in the measured spectrum and the fat green dashed bars the fit. (Shot 44195, nonsustained breakdown.) Also shown as the fat cyan solid bars fluctuating by ± 0.1 eV around zero is the spectrum measured when 400 kW rf was launched into empty vacuum vessel.

generated by the 4 MW ICRH power coupled to the plasma in this shot.

The fast ion distribution shown as the solid curve in Fig. 3 is inferred from the spectrum in Fig. 2 by a generalized least squares fitting method (LSN), which accounts for uncertainties in plasma and system parameters (nuisance parameters) inferred from other diagnostics [20]. The forward model for fast ion CTS used in the fitting is based on a fully kinetic description of the scattering, including scattering from electron density, flux and field fluctuations, and with a fully electromagnetic description of the microscopic fluctuations [5,6]. The error bars indicate one standard deviation. There are considerable correlations in these uncertainties, which are close to model predictions [8].

There is evidence from neutron spectroscopy that ICRH generated fast ions in the 100 keV range in JET may be redistributed by sawteeth [21]. Other neutron spectroscopy studies at JET [22] indicate that beam ions are strongly affected while 1 MeV tritons suffer only modest redistribution at sawtooth collapses. Analysis of escaping neutrals (NPA) at TFTR [23,24] suggests that the fusion alpha population is strongly affected by sawteeth, while triton and ^3He burn-up studies at DIII-D [25] reached similar conclusions. These measurements are all somewhat indirect, making it difficult to draw hard conclusions.

The distribution represented by the solid curve in Fig. 3 was inferred from data recorded 20–260 ms following the

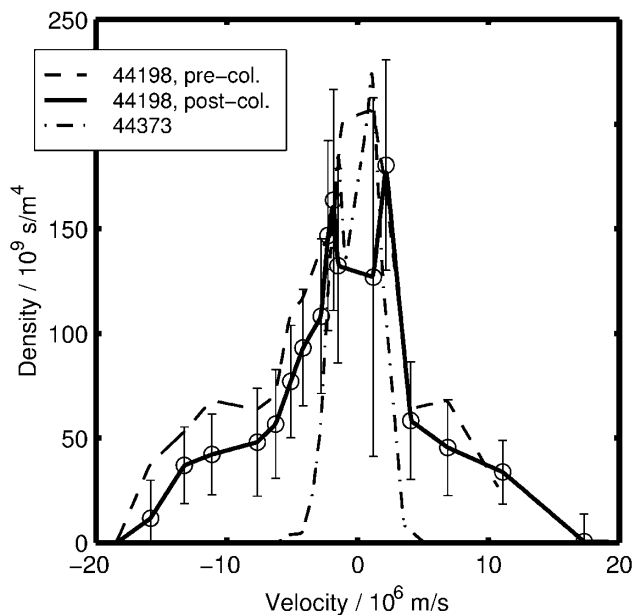


FIG. 3. The solid curve shows the 1D fast ion distribution, $f_H^{(1)}(u)$, inferred from CTS spectrum shown in Fig. 2, recorded for shot 44198 just after the sawtooth collapse at 12.725 sec after breakdown. $N_{H\text{fast}} = 2.0 \pm 0.36 \times 10^{18} \text{ m}^{-3}$. The dashed curve is the distribution inferred from the spectrum recorded just before the sawtooth collapse. The dash-dotted curve is the inferred fast ion distribution from CTS spectrum recorded in pulse 44373 and shown in Fig. 4. The error bars for this distribution are approximately twice those for 44198.

sawtooth collapse at 0.225 sec, while that represented by the dashed curve was inferred from the data recorded in the 230 ms before that collapse. The postcollapse distribution is 30% to 50% below the precollapse distribution, consistent with earlier indications of fast ion redistribution. More spurious gyrotron modes were present in the period preceding the crash, increasing the uncertainty in the measurement in this period. The difference between pre- and postcollapse distributions is thus on the margin of being significant.

In this shot $\phi = \angle(\mathbf{k}^\delta, \mathbf{B}^{(0)}) = 102^\circ$. Here $\mathbf{B}^{(0)}$ is the static magnetic field and \mathbf{k}^δ is the wave vector of the resolved fluctuations. With $u = \mathbf{v} \cdot \hat{\mathbf{k}}^\delta$ the resolved velocity component, the measured 1D distribution is $f_H^{(1)}(u) = \int f_H(\mathbf{v}) \delta(u - \hat{\mathbf{k}}^\delta \cdot \mathbf{v}) d^3\mathbf{v}$, so here we are mainly seeing the velocity components perpendicular to $\mathbf{B}^{(0)}$. The center of the scattering volume, and thus the location of the measurement, is estimated by ray tracing to be at $R_{\text{CTS}} = 3.14 \text{ m}$, $z = 0.26 \text{ m}$ (magnetic axis is at $R = 2.96 \text{ m}$). The ICRH frequencies were 51.11 to 51.32 MHz for which the minority hydrogen population has fundamental cyclotron resonances at $R_{\text{ICRH}} = 3.06$ to 3.07 m. The measurement is thus slightly to the low field side of the ICRH rf power deposition. The total density of fast protons (above thermal energy) is estimated at $2.0 \times 10^{18} \text{ m}^{-3}$ with a relative accuracy of 18%. This represents approximately 6% of the electron density. With no beam present in this shot, there is no other measurement of the hydrogen minority concentration. Plasma operation aimed for a minority H concentration of 5%. The fast ion energy density is estimated at $1.5 \times 10^5 \text{ J/m}^3$ with a relative uncertainty of 35%.

In Fig. 4 we show the recorded spectrum from plasma shot 44373. Here the power of the probing radiation was reduced to 100 kW and the detector noise increased due to modifications to attenuate stray radiation, hence the reduced signal-to-noise ratio. With $\phi = 119^\circ$ we are again mainly resolving the velocity components perpendicular to $\mathbf{B}^{(0)}$. The center of the scattering volume was estimated to be at $R_{\text{CTS}} = 3.09 \text{ m}$, $z = 0.28 \text{ m}$ while the ICRH frequencies were 51.05 to 51.33 MHz corresponding to fundamental hydrogen resonances at $R_{\text{ICRH}} = 3.10$ to 3.11 m. The difference between R_{CTS} and R_{ICRH} is within the uncertainties of either, but it does suggest that it is possible that the measurement was taken on the high field side of the ICRH rf power deposition. This would be consistent with the noticeable reduction in the width of the spectrum which is also reflected in reduced width of the inferred velocity distribution shown as the dash-dotted curve in Fig. 3.

The spatial distribution of fast ions is predicted to fall off very rapidly on the high field side of the resonance, principally because heating is most effective for ions at the high field turning points of their drift orbits. The spatial distributions found in numerical simulations [26] can show gradient scale lengths of less than 10 cm. We note that the relative location of scattering volume and ICRH resonances is shifted by approximately 9 cm

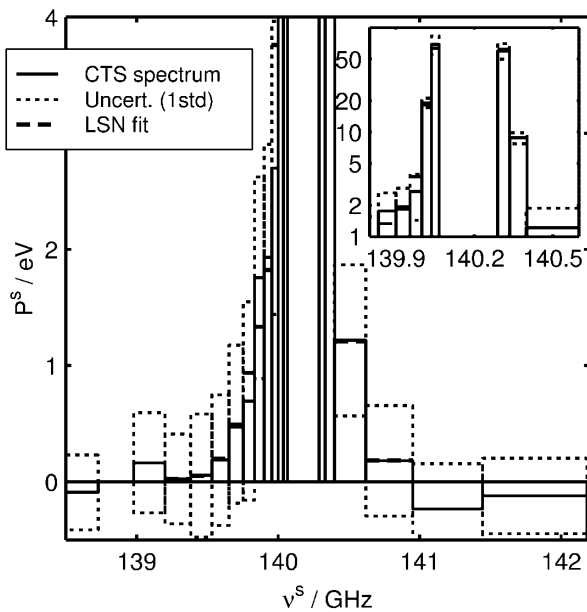


FIG. 4. Recorded spectrum when 100 kW rf launched into plasma. $P_{ICRH} = 4$ MW. $n_e = 3.9 \times 10^{19} \text{ m}^{-3}$, $T_e = 4.0$ keV, $T_i = 3.0$ keV, $\theta = 24^\circ$, $\phi = 119^\circ$. $N_{Hfast} = 0.9 \pm 0.5 \times 10^{18} \text{ m}^{-3}$. Inset shows spectral density in central channels.

towards the high-field side in shot 44373 compared with shot 44198 discussed above. It follows that the marked difference in distribution functions is not in conflict with theoretically predicted spatial gradients.

Conclusions.— We have demonstrated the feasibility of extracting an MeV range fast ion velocity distribution in an ICRH heated fusion plasma from spectral information obtained with collective Thomson scattering. The measured distribution differs significantly from the near Maxwellian distribution predicted by some models, which highlights the importance of direct and detailed measurements of the fast ion distribution. Significant spatial variation in the fast ion density on the high-field side of the rf absorption radius, consistent with modeling, is suggested. Fast MeV ion distributions were measured just before and after a saw-tooth collapse.

The resolution of the fast ion distribution, demonstrated here, already represents a significant new diagnostic capability, but is still far from the optimal performance of fast ion CTS. A range of technical problems could not be eliminated in the time available and had to be compensated for by modeling at the expense of resolution and accuracy of the inferred fast ion distributions. For the best shot, an integration time of only 30 ms was available, which may be compared with the 1000 ms pulses available from current gyrotrons, though the effective duration for a measurement may be limited to shorter times by changes in the plasma. Fully developed, this diagnostic can provide a valuable diagnostic capability for investigating fast ion distributions generated by ICRH. With this, both issues on ICRH physics and fast ion dynamics can be addressed.

We would like to thank Dr. P. Stott, Dr. P. Woskov, and Dr. M. Keilhacker, and the U.S. Department of

Energy for their continuing and highly valued support. Thanks are also extended to the ICRH group at JET.

*Now at FOM Instituut voor Plasmafysica “Rijnhuizen,” Postbus 1207, NL-3430 BE Nieuwegein, Netherlands.

Email address: bindslev@rijnh.nl

†Now at Forschungszentrum, IPP, D-52425 Jülich, Germany.

‡Now at MIT, PSFC, Cambridge, MA 02139.

§University of Essex, Colchester, United Kingdom.

||MIT, PSFC, Cambridge, MA 02139.

- [1] M. N. Rosenbluth and P. H. Rutherford, *Phys. Rev. Lett.* **34**, 1428 (1975).
- [2] W. Kerner *et al.*, *Nucl. Fusion* **38**, 1315 (1998).
- [3] A. Sitenko and Y. Kirochkin, *Sov. Phys. Usp.* **9**, 430 (1966).
- [4] R. Aamodt and D. Russell, *Nucl. Fusion* **32**, 745 (1992).
- [5] H. Bindslev, *J. Atmos. Terr. Phys.* **58**, 983 (1996).
- [6] H. Bindslev, *Plasma Phys. Controlled Fusion* **35**, 1615 (1993).
- [7] H. Bindslev, in *Proceedings of the 3rd International Workshop on Strong Microwaves in Plasmas, Volga 1996*, edited by A. G. Litvak (Russian Academy of Sciences, Institute of Applied Physics, Nizhny Novgorod, 1996), pp. 109–128.
- [8] H. Bindslev, in *Proceedings of the 8th International Symposium on Laser-Aided Plasma Diagnostics, Doorvert 1997*, edited by A. J. H. Donné (FOM “Rijnhuizen,” Nieuwegein, Netherlands, 1997), pp. 265–276.
- [9] R. Behn *et al.*, *Phys. Rev. Lett.* **62**, 2833 (1989).
- [10] J. A. Hoekzema *et al.*, in *Proceedings of the 22nd EPS Conference on Controlled Fusion and Plasma Physics, Bournemouth, 1995*, edited by B. E. Keen *et al.* (European Physical Society, Geneva, 1995).
- [11] J. A. Hoekzema *et al.*, *Rev. Sci. Instrum.* **68**, 275 (1997).
- [12] J. A. Hoekzema *et al.*, in *Proceedings of the 7th International Symposium on Laser-Aided Plasma Diagnostics Fukuoka 1995*, edited by K. Muraoka (Kyushu University, Fukuoka, Japan, 1995), p. 166.
- [13] H. Bindslev *et al.*, in *Proceedings of the 3rd International Workshop on Strong Microwaves in Plasmas, Volga 1996* (Ref. [7]), pp. 142–165.
- [14] E. V. Suvorov *et al.*, *Plasma Phys. Controlled Fusion* **37**, 1207 (1995).
- [15] P. Woskoboinikow, *Rev. Sci. Instrum.* **57**, 2113 (1986).
- [16] T. P. Hughes, H. Bindslev, J. Egedal, and J. A. Hoekzema, in *Proceedings of EC-10, Ameland 1997* (World Scientific, Singapore, 1997), p. 277.
- [17] The JET Team, J. Jacquinot *et al.*, in *Proceedings of the 16th International Conference on Fusion Energy, Montreal 1996* (IAEA, Vienna, 1997), Vol. 1, p. 57.
- [18] J. Egedal *et al.*, *Rev. Sci. Instrum.* **70**, 1167 (1999).
- [19] J. S. Machuzak *et al.*, *Rev. Sci. Instrum.* **70**, 1154 (1999).
- [20] H. Bindslev *Rev. Sci. Instrum.* **70**, 1093 (1999).
- [21] D. F. H. Start *et al.*, *Phys. Rev. Lett.* **80**, 4681 (1998).
- [22] F. B. Marcus *et al.*, *Nucl. Fusion* **34**, 687 (1994).
- [23] R. K. Fisher *et al.*, *Phys. Rev. Lett.* **75**, 846 (1995).
- [24] M. P. Petrov *et al.*, *Nucl. Fusion* **35**, 1437 (1995).
- [25] H. H. Duong and W. W. Heidbrink, *Nucl. Fusion* **33**, 211 (1993).
- [26] L.-G. Eriksson *et al.*, *Phys. Rev. Lett.* **81**, 1231 (1998).